

Preparation of an emittance transfer experiment

C. Xiao and O. Kester

Institut Angewandte Physik, Goethe-Universität Frankfurt, Frankfurt am Main D60438, Germany

L. Groening, H. Leibrock, and M. Maier

GSI Helmholtzzentrum für Schwerionenforschung GmbH, Darmstadt D64291, Germany

(Dated: July 22, 2018)

Flat beams feature unequal emittances in the horizontal and vertical phase space. Those beams were created successfully in lepton machines. Although a number of applications will profit also from flat hadron beams, to our knowledge they have never been created systematically. Multi-turn injection schemes, spectrometers, and colliders will directly benefit from those beams. The present paper covers the preparation of the experimental proof of principle for flat hadron beam creation in a beam transport section. Detailed simulations of the experiment, based on charge state stripping inside of a solenoid [L. Groening, *Phys. Rev. ST Accel. Beams* 14, 064201 (2011)], are performed. The matrix formalism was benchmarked with tracking through three-dimensional magnetic field maps of solenoids. An error analysis targeting at investigation of the impact of machine errors on the round-to-flat beam transformation has been performed. The remarkable flexibility of the set-up w.r.t. decoupling is addressed, as it can provide a one-knob tool to set the horizontal and vertical emittance partitioning. Finally, the status of hardware design and production is given.

PACS numbers: 41.75.Ak, 41.85.Ct, 41.85.Ja

I. INTRODUCTION

The modification of projected beam emittances under preservation of the full six-dimensional emittance became a matter of interest for many accelerator applications. First experiments were proposed and conducted by D. Edwards et al. [1] for electron machines about a decade ago. The issue is of special interest for increasing the performance of X-FELs and advanced approaches to emittance repartitioning are under conceptual and experimental investigation [2–6]. Flat hadron beams could facilitate the process of multi-turn injection into circular machines, which imposes different requirements on the horizontal and vertical emittance of the incoming beam. Recently it was proposed to use flat beams in hadron-hadron collisions to provide higher luminosity by mitigating beam-beam effects [7]. The mass resolution of spectrometers is increased significantly if the beam is flat perpendicular to the direction of the spectrometers bend. A corresponding set-up behind an Electron-Cyclotron-Resonance source is proposed in [8].

From first principles beams are created round without any coupling among planes. Their rms emittances as well as their eigen-emittances are equal in the two transverse planes. Thus, any transverse round-to-flat transformation requires a change of the beam eigen-emittances by a non-symplectic transformation [9]. Such a transformation can be performed by placing a charge state stripper inside an axial magnetic field region as proposed in [10]. Inside such a solenoid stripper, transverse inter-plane correlations are created non-symplectically. Afterwards they are removed symplectically by a decoupling section including skew quadrupoles. It must be mentioned that the use of charge state strippers (outside from solenoids) is state-of-the art at several ion machines that provide

highly charged ions.

It is emphasized that the paper is on the application of coupled beam dynamics aiming for increased performance of an accelerator chain. It is not on coupled beam dynamics theory itself and references are given whenever needed. The paper starts with a re-introduction of the required terms of coupled beam dynamics. Afterwards the new set-up for experimental demonstration of transverse emittance transfer is introduced. The fourth section is on modeling the non-symplectic process of charge state stripping inside a solenoid. Results from models based on matrix formalism are benchmarked with those from tracking particles through three-dimensional field maps derived from magnet design codes. Such benchmarks were made for different finite fringe field shapes of the solenoid. Afterwards, the symplectic decoupling section is treated. The sixth section analyses the impact of machine errors on the decoupling performance of the beam line. It was found that the decoupling capability of the set-up is remarkably flexible and the impact and discussion of this finding is treated in a dedicated section. The paper closes with some conclusions and an outlook w.r.t. procurement of the required hardware.

II. BASIC TERMS

The four-dimensional symmetric beam matrix C contains ten unique elements, four of which describe the coupling. If one or more of the elements of the off-diagonal sub-matrix is non-zero, the beam is x - y coupled:

$$C = \begin{bmatrix} \langle xx \rangle & \langle xx' \rangle & \langle xy \rangle & \langle xy' \rangle \\ \langle x'x \rangle & \langle x'x' \rangle & \langle x'y \rangle & \langle x'y' \rangle \\ \langle yx \rangle & \langle yx' \rangle & \langle yy \rangle & \langle yy' \rangle \\ \langle y'x \rangle & \langle y'x' \rangle & \langle y'y \rangle & \langle y'y' \rangle \end{bmatrix}. \quad (1)$$

The four-dimensional rms emittance ε_{4d} is the square root of the determinant of C , and the projected beam rms emittances ε_x and ε_y are the square roots of the determinants of the on-diagonal sub-matrices. Diagonalization of the beam matrix yields the eigen-emittances ε_1 and ε_2 which are calculated as

$$\varepsilon_{1,2} = \frac{1}{2} \sqrt{-\text{tr}(CJ)^2 \pm \sqrt{\text{tr}^2(CJ)^2 - 16\text{det}(C)}}. \quad (2)$$

The four-dimensional matrix J is the skew-symmetric matrix with non-zero entries on the block diagonal off form. Any symplectic transformation M obeys

$$M^T J M = J, \quad J = \begin{bmatrix} 0 & 1 & 0 & 0 \\ -1 & 0 & 0 & 0 \\ 0 & 0 & 0 & 1 \\ 0 & 0 & -1 & 0 \end{bmatrix}. \quad (3)$$

Eigen-emittances are invariant under symplectic transformations and the eigen-emittances are equal to the rms emittances only if inter-plane (x - y) correlations are zero.

III. EXPERIMENTAL SET-UP

The new EMTEX (emittance transfer experiment) beam line for the demonstration of transverse emittance transfer is shown in Fig. 1 and it will be integrated into the existing transfer line from the UNILAC [11] to the SIS-18 synchrotron.

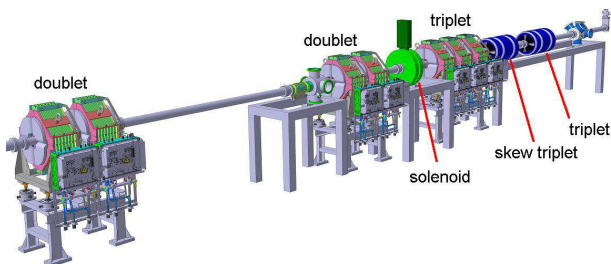


FIG. 1. The layout of the EMTEX section at GSI.

The transverse emittance transfer beam line comprises two quadrupole doublets, a solenoid with stripper foil inside, a quadrupole triplet, a skew quadrupole triplet, another quadrupole triplet, a current transformer, and a transverse emittance measurement unit. Its total length is 12785 mm.

In order to mitigate four-dimensional rms emittance growth from scattering during the stripping process, the beam sizes at the stripper should be kept small. Two quadrupole doublets separated by a drift space in front of the solenoid do the required matching. The maximum gradients of the quadrupole magnets are 19.0 and 15.0 T/m and the effective field lengths are 319 and 354 mm, respectively. A low intensity beam of D_6^+ stripped to $3D_2^+$ in a $20 \mu\text{g}/\text{cm}^2$ carbon foil placed at the

center of a solenoid will be used, and the total relative momentum spread of the beam is less than $\pm 5 \times 10^{-4}$. The maximum longitudinal magnetic field is 1.0 T. This non-symplectic transformation creates coupling between the two transverse planes [12]. A quadrupole triplet and a skew quadrupole triplet separated by a drift space are employed to remove these correlation symplectically. It will be called decoupling section in the following. A final quadrupole triplet is used for matching to the existing beam line followed by a beam current transformer and an emittance measurement unit. The full beam line is presented quantitatively in the Appendix.

IV. STRIPPING INSIDE A SOLENOID

Stripping inside a solenoid is fundamentally different from stripping between two solenoids due to the longitudinal magnetic field component and the fringe fields. In case of pure transverse field components (dipoles, quadrupoles, n-poles) there is equivalence between stripping inside this magnet and stripping between two such magnets of half lengths.

Let C_0 denote the second moment matrix at the entrance of the solenoid. If the beam has equal horizontal and vertical rms emittances, the beam matrix can be simplified to

$$C_0 = \begin{bmatrix} \varepsilon\beta & 0 & 0 & 0 \\ 0 & \frac{\varepsilon}{\beta} & 0 & 0 \\ 0 & 0 & \varepsilon\beta & 0 \\ 0 & 0 & 0 & \frac{\varepsilon}{\beta} \end{bmatrix}. \quad (4)$$

Assuming a very short solenoid, its transport matrix can be divided into two parts

$$R_{in} = \begin{bmatrix} 1 & 0 & 0 & 0 \\ 0 & 1 & k_{in} & 0 \\ 0 & 0 & 1 & 0 \\ -k_{in} & 0 & 0 & 1 \end{bmatrix}, \quad R_{out} = \begin{bmatrix} 1 & 0 & 0 & 0 \\ 0 & 1 & -k_{out} & 0 \\ 0 & 0 & 1 & 0 \\ k_{out} & 0 & 0 & 1 \end{bmatrix}. \quad (5)$$

If the beam has the same energy and charge state at the solenoid entrance and exit, k_{in} is equal to k_{out} . The first part describes the entrance fringe field and the second part is the exit fringe field. In here, the focusing strength of the solenoid is

$$k = \frac{B}{2(B\rho)}. \quad (6)$$

B is the on-axis magnetic field strength, and $B\rho$ is the beam rigidity. The beam matrix C_1 after the entrance fringe field k is found in the following form

$$C_1 = R_{in} C_0 R_{in}^T = \begin{bmatrix} \varepsilon\beta & 0 & 0 & -k\varepsilon\beta \\ 0 & \frac{\varepsilon}{\beta} + k^2\varepsilon\beta & k\varepsilon\beta & 0 \\ 0 & k\varepsilon\beta & \varepsilon\beta & 0 \\ -k\varepsilon\beta & 0 & 0 & \frac{\varepsilon}{\beta} + k^2\varepsilon\beta \end{bmatrix}. \quad (7)$$

The off-diagonal sub-matrices describe the correlations and the values of $\langle xy \rangle$ and $\langle x'y' \rangle$ are zero. In order to achieve a change of the eigen-emittances a non-symplectic transformation has to be integrated into the round-to-flat transformation section. The transformation through the solenoid is non-symplectic if the beam rigidity is abruptly changed in between the entrance and exit fringe fields, thus the beam properties are reset inside the solenoid. The non-symplectic transformation is accomplished by using a beam of D_6^+ stripped to $3D_2^+$ in a carbon foil placed at the center of solenoid. Thus, the exit fringe field transfer matrix is changed to:

$$R'_{out} = \begin{bmatrix} 1 & 0 & 0 & 0 \\ 0 & 1 & -3k & 0 \\ 0 & 0 & 1 & 0 \\ 3k & 0 & 0 & 1 \end{bmatrix}. \quad (8)$$

The focusing strength of the solenoid k is calculated from the unstripped charge state. The elements of the beam matrix C'_1 directly after the stripper inside of the solenoid but still before the exit fringe field are

$$C'_1 = \begin{bmatrix} \varepsilon\beta & 0 & 0 & -k\varepsilon\beta \\ 0 & \frac{\varepsilon}{\beta} + k^2\varepsilon\beta + \Delta\varphi^2 & k\varepsilon\beta & 0 \\ 0 & k\varepsilon\beta & \varepsilon\beta & 0 \\ -k\varepsilon\beta & 0 & 0 & \frac{\varepsilon}{\beta} + k^2\varepsilon\beta + \Delta\varphi^2 \end{bmatrix}. \quad (9)$$

The stripper scattering effects on the angular spread are included. The energy loss and straggling in the stripper foil can be neglected in our case. The parameter $\Delta\varphi^2$ is the scattering amount during the stripping process [13], and the foil stripper itself is modeled by increasing the spread of the angular distribution through scattering. After the stripper the beam passes through the exit fringe field with reduced beam rigidity and the beam matrix C'_2 after the exit fringe field becomes

$$C'_2 = R'_{out} C'_1 R'^T_{out} = \begin{bmatrix} \varepsilon_n R_n & 2k\varepsilon_n \beta_n J_n \\ -2k\varepsilon_n \beta_n J_n & \varepsilon_n R_n \end{bmatrix}, \quad (10)$$

where

$$\varepsilon_n = \sqrt{\varepsilon\beta\left(\frac{\varepsilon}{\beta} + 4k^2\varepsilon\beta + \Delta\varphi^2\right)}, \quad \beta_n = \frac{\beta\varepsilon}{\varepsilon_n}, \quad (11)$$

introducing the 2×2 sub-matrices R_n and J_n as

$$R_n = \begin{bmatrix} \beta_n & 0 \\ 0 & \frac{1}{\beta_n} \end{bmatrix}, \quad J_n = \begin{bmatrix} 0 & 1 \\ -1 & 0 \end{bmatrix}. \quad (12)$$

The amount of eigen-emittance transfer scales with the longitudinal magnetic field strength and the beam rms sizes on the stripper. Inter-plane correlations are created and the rms emittances and eigen-emittances after the solenoid with stripper foil can be written as:

$$\varepsilon_{x,y} = \varepsilon_n, \quad \varepsilon_{1,2} = \varepsilon_n(1 \pm 2k\beta_n). \quad (13)$$

The four-dimensional rms emittance can be written as

$$\varepsilon_{4d} = \varepsilon_1 \varepsilon_2 = \varepsilon^2 + \varepsilon\beta\Delta\varphi^2. \quad (14)$$

The value of the four-dimensional rms emittance increase is proportional to the square of beam sizes on the stripper. The increase is purely from scattering in the foil, it is not caused by the shift of beam rigidity inside the longitudinal magnetic field. The evolutions of the rms emittances and the eigen-emittances along a solenoid channel which is composed of two drift space separated by a solenoid are shown in Fig. 2. For the beam transport through the solenoid, the linear solenoid transfer matrix is used and the stripper foil is placed at the solenoid center. Once the beam feels the entrance fringe, the eigen-emittances start to split out rapidly and do not change until the stripper foil. Taking into account the scattering in the stripper foil, the eigen-emittances increase abruptly during the stripping process. After stripping, the exit fringe is passed by the beam with reduced rigidity, thus overcompensating the previous eigen-emittance variations. The fringe fields of the solenoid, rather than the pure longitudinal magnetic field, cause the change of eigen-emittances.

Multi-particle tracking in the proposed transverse emittance transfer section is done with the TRACK code [14].

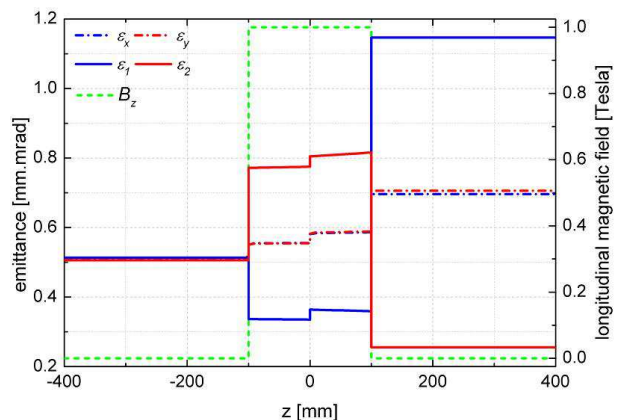


FIG. 2. Evolutions of rms emittances and eigen-emittances along the solenoid channel using a transfer matrix.

By variations of the aperture size of solenoid, the effective length of the solenoid is constant and the transfer matrix will remain unchanged, while the actual three-dimensional field map will be affected. In order to verify whether usage of the transfer matrix formalism is justified, it was compared with tracking simulations for two different solenoids of equal effective field length but with different fringe field shapes obtained from three-dimensional field maps of the OPERA-3D finite element code [15]. The evolutions of rms emittances and eigen-emittances along solenoids with different aperture radii are shown in Fig. 3. The solenoids effective lengths are set to 200 mm, and the solenoids aperture radii are chosen to be 30 and 90 mm, respectively.

Additionally we treated the case of fixed solenoid aperture radius but different effective field lengths. The evolutions of the rms emittances and eigen-emittances along

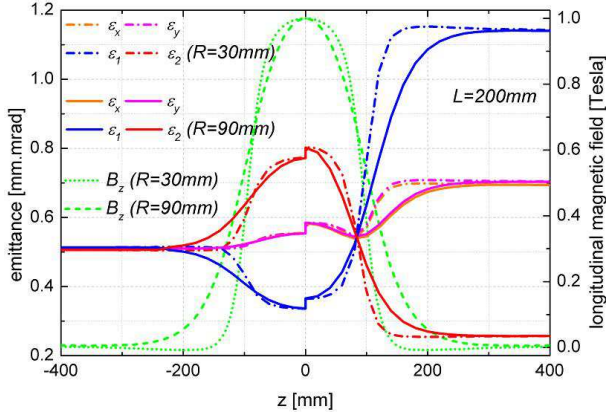


FIG. 3. Evolutions of rms emittances and eigen-emittances along the solenoid, with same effective lengths but different aperture radii. The results are from tracking through three-dimensional magnetic field maps.

solenoids with different effective field lengths are shown in Fig. 4. In this simulation, the solenoid aperture radius is set to 60 mm, and the solenoid effective lengths are chosen 200 and 300 mm, respectively.

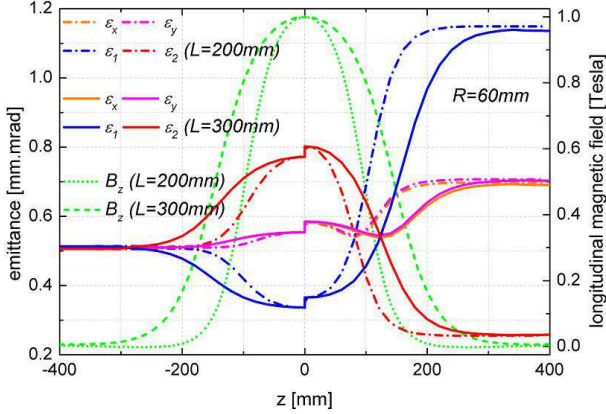


FIG. 4. Evolutions of rms emittances and eigen-emittances along the solenoid, with identical inner radius but different effective lengths. The results are from tracking through three-dimensional magnetic field maps.

The simulations demonstrated that the treatment of the solenoidal stripping process with linear matrices as initially done in [10] is justified. The final rms emittances and eigen-emittances do not depend on the exact shape of the fringe field as long as it is reasonably short like for the solenoids that are commonly in use. Additional material on this issue can be found in [16, 17].

V. DECOUPLING SECTION

The simplest skew decoupling section contains three skew quadrupoles with appropriate betatron phase advances in each plane [18, 19]. Let R_q be the 4×4 matrix

corresponding to a certain arrangement of quadrupoles and drift spaces and assume that this channel is represented by an identity matrix in the x -direction and has an additional 90° phase advance in y -direction as in [20]

$$R_q = \begin{bmatrix} I_n & O_n \\ O_n & T_n \end{bmatrix}. \quad (15)$$

Here the 2×2 sub-matrices O_n , T_n and I_n are defined as

$$O_n = \begin{bmatrix} 0 & 0 \\ 0 & 0 \end{bmatrix}, \quad T_n = \begin{bmatrix} 0 & U \\ -\frac{1}{U} & 0 \end{bmatrix}, \quad I_n = \begin{bmatrix} 1 & 0 \\ 0 & 1 \end{bmatrix}. \quad (16)$$

If the quadrupoles are tilted by 45° the 4×4 transfer matrix can be written as

$$\bar{R} = R_r R_q R_r^T = \frac{1}{2} \begin{bmatrix} T_{n+} & T_{n-} \\ T_{n-} & T_{n+} \end{bmatrix}, \quad (17)$$

where

$$R_r = \frac{\sqrt{2}}{2} \begin{bmatrix} I_n & I_n \\ -I_n & I_n \end{bmatrix}, \quad T_{n\pm} = T_n \pm I_n. \quad (18)$$

The beam matrix C'_3 after the decoupling section is

$$C'_3 = \bar{R} C'_2 \bar{R}^T = \begin{bmatrix} \eta_+ \Gamma_{n+} & \zeta \Gamma_{n-} \\ \zeta \Gamma_{n-} & \eta_- \Gamma_{n+} \end{bmatrix}, \quad (19)$$

and the 2×2 sub-matrices $\Gamma_{n\pm}$ are defined through

$$\Gamma_{n\pm} = \begin{bmatrix} U & 0 \\ 0 & \pm \frac{1}{U} \end{bmatrix}, \quad (20)$$

with

$$\eta_{\pm} = \frac{\varepsilon_n}{2} \left(\frac{\beta_n}{U} + \frac{U}{\beta_n} \pm 4k\beta_n \right), \quad (21)$$

and

$$\zeta = \frac{\varepsilon_n}{2} \left(-\frac{\beta_n}{U} + \frac{U}{\beta_n} \right). \quad (22)$$

Assuming that this beam matrix is diagonal, its x - y component vanishes

$$\zeta \Gamma_{n-} = O_n. \quad (23)$$

This equation is solved by

$$U = \beta_n. \quad (24)$$

This result was found earlier in [20] for instance. However, the major steps have been repeated here since they will be referred to later.

Suppose that the decoupling transfer matrix \bar{R} is able to decouple the two transverse planes of C'_2 . We still do not know how this transfer beam line looks in detail, but anyway we calculate the final rms emittances obtaining

$$\varepsilon_{x,y} = \frac{\varepsilon_n}{2} \left(\frac{\beta_n}{U} + \frac{U}{\beta_n} \pm 4k\beta_n \right). \quad (25)$$

This idealized example serves illustrating the principle, and it may be accomplished with just three skew quadrupoles. In our design, more elements are used because of finite apertures and gradients of a real experiment. In our set-up the decoupling section comprises a quadrupole triplet and a skew quadrupole triplet separated by a drift. The quadrupole gradients are optimized numerically from a numerical routine [10] to remove the inter-plane correlations thus minimizing the horizontal (for instance) rms emittances to the lower of the eigen-emittances.

Fig. 5 illustrates the transverse emittance transfer. In the first step we assume that we turn off the power supplies of the solenoid and the skew quadrupole triplet. This process is an ordinary stripping process and the eigen-emittances are equal to the rms emittances at the exit of this section. It reflects today's situation of providing highly charged ions from linacs. Due to the stripping, growth of eigen-emittances and rms emittances is unavoidable. It is the reference scenario to which the emittance transfer scenario is to be compared. In the latter the solenoid field and the decoupling skew quads are turned on. The eigen-emittances diverge inside the solenoid but they are preserved afterwards. Along the decoupling skew quadrupole triplet the rms emittances are made equal to the diverged eigen-emittances. Compared to the reference scenario, the final horizontal rms emittance is reduced significantly by a factor two. This emittance transfer experiment (EMTEX) is therefore fundamentally different from an emittance exchange experiment (EEX). EMTX is non-symplectic and the amount of transfer can be controlled by the solenoid field strength and/or the beam size on the stripping foil.

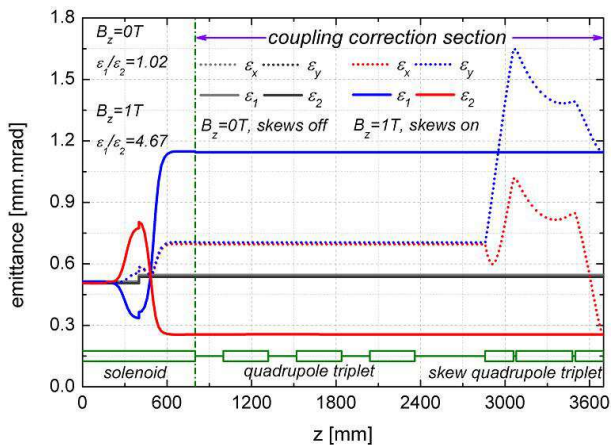


FIG. 5. Evolution of rms emittances and eigen-emittances along the longitudinal magnetic field and the decoupling section for two scenarios: solenoid and skew quads off (reference, green and dark green lines); solenoid and skew quads on (emittance transfer), $B_z=1.00$ T.

Behind the decoupling section another quadrupole triplet is required to rematch the beam for further transport to

the SIS-18 synchrotron. The beam rms sizes along the total beam line are shown in Fig. 6 (solenoid and skew quads on) and the particle distributions at the exit of beam line are illustrated in Fig. 7.

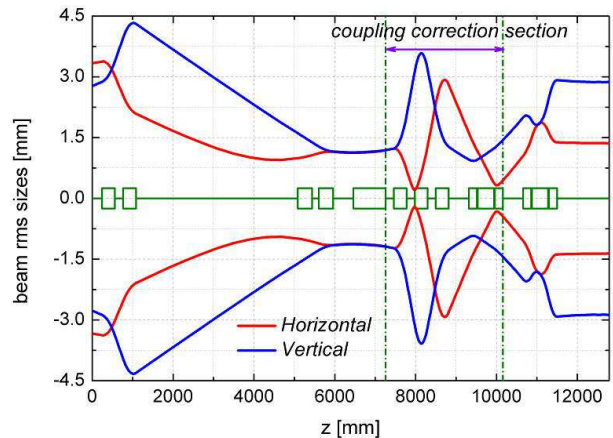


FIG. 6. Horizontal and vertical beam rms sizes along the proposed transverse emittance transfer section.

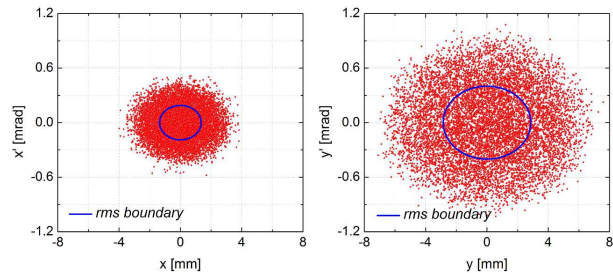


FIG. 7. The transverse emittance portraits at the exit of proposed transverse emittance transfer section.

VI. ERROR STUDIES

The decoupling of the transverse planes is sensitive to machine errors. Alignment failures and/or gradient errors directly enter into the transformations and flaw the decoupling performance. In order to quantify the impact of such errors on the experiment, dedicated error studies were done w.r.t. gradient errors and rolls of quadrupoles. Gradient deviations and rolls were distributed randomly among all magnets of the set-up. Different error distributions were used to simulate the experiment by tracking. The influence of gradient fluctuations and rolls on the final horizontal rms emittance and lower eigen-emittances are shown in Fig. 8. Based on the experiences of the UNILAC, the maximum values of gradient fluctuations and rolls can be kept below 0.1% and 0.3°, respectively.

It turned out that the gradient fluctuations are not crit-

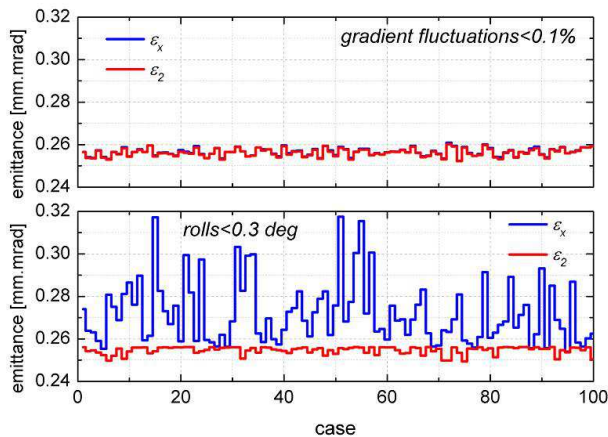


FIG. 8. Influence of gradient fluctuations and magnet rolls on the horizontal rms emittance and lower eigen-emittances.

ical. In case of rolls, the values of horizontal rms emittances are larger than the lower eigen-emittances, indicating incomplete decoupling. The related beam line errors degrade the accuracy of decoupling. Assuming that the gradient fluctuations and rotational angles are lower than $\pm 0.1\%$ and 0.3° , it does just slightly harm the decoupling capability, i.e. the coupling elements are removed sufficiently well.

VII. DECOUPLING CAPABILITY ANALYSIS

The parameter t is introduced to quantify the inter-plane coupling. If t defined as

$$t = \frac{\epsilon_x \epsilon_y}{\epsilon_1 \epsilon_2} - 1 \quad (26)$$

is equal to zero, there are no inter-plane correlations and the beam is fully decoupled. Kim [20] introduced the beam angular momentum $2\xi = \langle xy' - x'y \rangle$ and for an angular momentum dominated beam one finds $t = \xi^2 / \epsilon_{4d}$. For a given solenoid strength k_0 , referring to the unstripped beam, the corresponding quadrupole gradients of the decoupling section are determined using a numerical routine, such that finally the rms emittances are equal to the eigen-emittances. If these optimized gradients are applied to remove inter-plane correlations produced by a different solenoid strength k_1 , the resulting rms emittances and eigen-emittances at the exit of the decoupling section are calculated to be

$$\epsilon_{x,y} = \frac{\epsilon_n(k_1)}{2} \left[\frac{\beta_n(k_1)}{\beta_n(k_0)} + \frac{\beta_n(k_0)}{\beta_n(k_1)} \pm 4k_1 \beta_n(k_1) \right], \quad (27)$$

and

$$\epsilon_{1,2} = \epsilon_n(k_1) [1 \pm 2k_1 \beta_n(k_1)]. \quad (28)$$

The parameter t is then

$$t = \frac{4\epsilon^2 \beta^2}{\left(\frac{\epsilon}{\beta} + \Delta\varphi^2\right) \left(\frac{\epsilon}{\beta} + 4k_0^2 \epsilon \beta + \Delta\varphi^2\right)} (k_1^2 - k_0^2)^2. \quad (29)$$

In the experiment, we will have a beam of molecules from D_6^+ with the initial beam parameters $\alpha=0$, $\beta=2.5$ mm/mrad and $\epsilon=0.51$ mm.mrad at the entrance of the solenoid. The stripping scattering amount $\Delta\varphi$ is 0.226 mrad [13] and the decoupling transfer matrix is determined for 1.0 T of solenoid field. For the simplest decoupling transfer matrix, the decoupling section is a skew quadrupole triplet. In our case, the decoupling section comprises a quadrupole triplet and a skew quadrupole triplet separated by a drift. Therefore, our decoupling transfer matrix has a more complex structure, explicitly (in units of mm mrad)

$$\bar{R}' = \begin{bmatrix} -0.9224 & 1.6051 & -0.4133 & -0.4703 \\ -0.7274 & 0.2415 & -1.6969 & -2.0649 \\ 0.0746 & -0.2830 & 2.9308 & 3.6770 \\ 0.4603 & -1.0047 & 1.1329 & 1.7437 \end{bmatrix}, \quad (30)$$

being different from the form used in Eq. (17). The final eigen-emittances and rms emittances calculated using Eq. (17) and those obtained from tracking through our specific set-up are compared in Fig. 9. For the

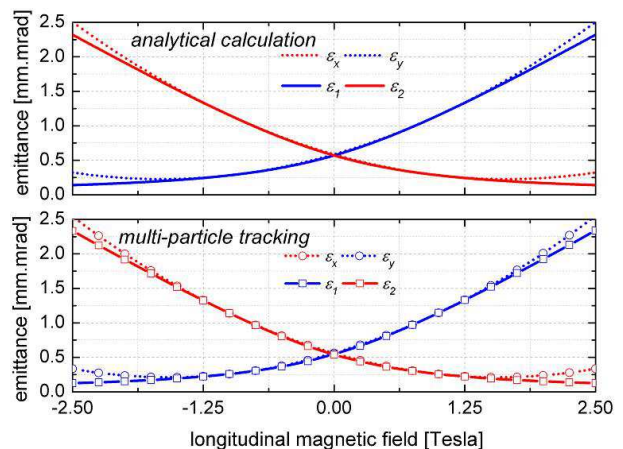


FIG. 9. Eigen-emittances and rms emittances calculated by analytical method based on the decoupling matrix of Eq. (17) and by multi-particle tracking through our specific set-up. Although the longitudinal magnetic field is varied, the decoupling gradients are kept constant at the values determined to decouple the beam coupled by a longitudinal magnetic field of 1 T.

simple decoupling section the calculation is based on the transfer matrix method of Eq. (17). For our decoupling section multi-particle tracking through the external three-dimensional field maps (for the solenoid) and the external one-dimensional field profile (for the quadrupole and skew quadrupole) were adopted.

The remarkable result is that both decoupling matrices work effectively for a wide range of longitudinal magnetic field values, i.e. the beam is well decoupled for a wide range of longitudinal magnetic fields around the gradients of the decoupling section the quadrupoles have been optimized for. Additionally, in both cases the

decoupling performance is independent from the sign of k_1 as suggested by Eq. (29) and weakly depended on k_1-k_0 . We currently do not have a complete analytical understanding of this weak dependence except for the simple decoupling matrix Eq (17). However, we still aim for understanding why the dependence is so weak even for our decoupling line being more complex w.r.t. the form of Eq. (17). To exclude that this is casual for this one beam line, the beam line has been modified by prolonging or shortening drifts and quadrupole field lengths. For all modifications (all using a regular quadrupole triplet followed by a skew quadrupole triplet) the same behavior of the decoupling performance was observed.

However, this behavior simplifies the decoupling significantly as re-adoption of gradients to the solenoid field can be skipped within a reasonable range of solenoid fields. It provides an one-knob set-up to partition the horizontal and vertical beam rms emittances. The behavior of t calculated by the analytical method based on Eq. (17) and on tracking through our set-up is illustrated in Fig. 10, where the stripping scattering amount $\Delta\varphi$ is set to 0.226 mrad and the longitudinal magnetic field is varied. In our set-up k_0 corresponds to a solenoid field of 1 T and accordingly t has a minimum for that value. The beam is well decoupled for a wide range of solenoid fields for both the analytical calculation and for tracking through the specific set-up.

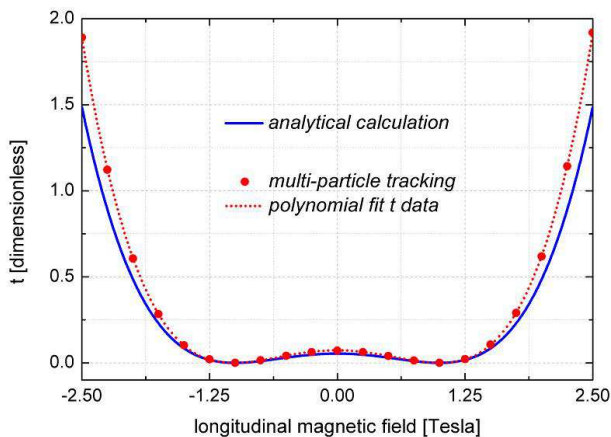


FIG. 10. The parameter t calculated by analytical method and multi-particle tracking simulation. Although the longitudinal magnetic field is varied, the decoupling gradients are kept constant at the values determined to decouple the beam coupled by a longitudinal magnetic field of 1 T.

The dependence of t on the solenoid field as obtained from tracking has been fitted with a 4th order polynomial as motivated by Eq. (29) and the fit is plotted as well in Fig. 10. This result might suggest a general 4th order dependence of the decoupling performance of any beam line on the coupling-driving solenoid field. The analytical investigation of this suggestion is beyond the

scope of this paper.

Finally we calculated the case of fixed longitudinal magnetic field but different stripping scattering amount $\Delta\varphi$, and the behavior of t simulated by multi-particle tracking through our set-up is illustrated in Fig. 11. The decoupling is also quite independent from the amount of scattering, which will additionally facilitate the experiment.

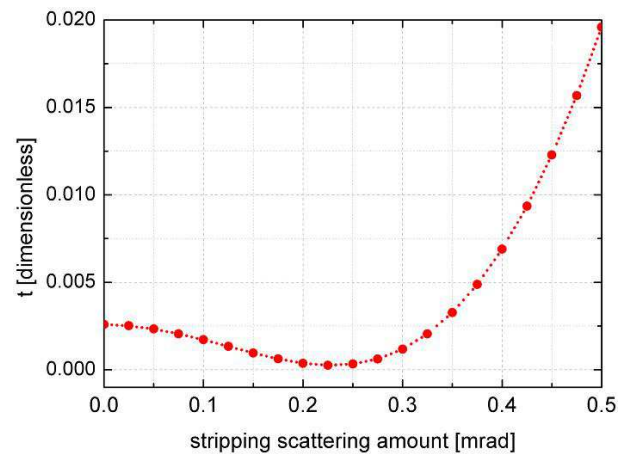


FIG. 11. The parameter t calculated by multi-particle tracking simulation as a function of the foil scattering angle. Although the scattering angle is varied, the decoupling gradients are kept constant at the values determined to decouple the beam coupled by a scattering angle of 0.226 mrad.

VIII. CONCLUSION AND OUTLOOK

An experimental set-up for demonstration of round-to-flat transformation of an initially decoupled ion beam was presented. It comprises two doublets for matching the required beam parameters on a stripping foil being placed in the center of a solenoid of about 1.0 T. The net effect on the beam is a non-symplectic transformation creating inter-plane coupling, being removed afterwards along a beam line from one regular quadrupole triplet and one skew quadrupole triplet. Extensive tracking simulations through three-dimensional field maps of the solenoid were performed for a variety of field shapes, showing excellent agreement to the pure matrix formalism. Angular scattering during stripping was included and an error study was performed. The latter revealed that quadrupole rolls may slightly but not significantly harm the decoupling performance. This decoupling performance was found to be very stable w.r.t. the field strength of the solenoid, i.e. the same decoupling gradients can be applied for a wide range of solenoid fields without relevant reduction of the decoupling performance. This remarkable result can be partially understood analytically. Apart from that it facilitates

the conduction of the experiment itself.

The beam line is currently under construction. Quadrupole triplets and doublets are on site or under production. Power converters were ordered and the installation of the infrastructure is scheduled. The solenoid, comprising two separate coils, including its chamber, which in turn houses the driver to move the stripping foil on the beam axis, is shown in Fig 12. The solenoid design avoids a local field minimum in the center, since it might act as a trap of electrons. All required diagnostic devices are already installed and operational. We currently plan to do the experiment in 2014, that work is supported by the HIC for FAIR and the BMBF.

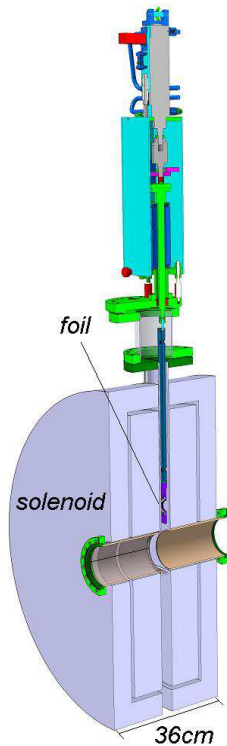


FIG. 12. The solenoid comprising two coils, its chamber, and the driver mechanics to place the stripping foil on the beam axis.

ACKNOWLEDGMENTS

The authors wish to express their gratitude to Brahim Mustapha at ANL, and Ina Pschorn at GSI for fruitful discussions.

Appendix A

The beam parameters at the entrance and exit of the beam line are listed in Tab. I. A D_6^+ beam of 11.4

TABLE I. The beam parameters at the entrance and exit of the EMTEX beam line.

Parameters	Entrance	Exit
α_x/α_y	-1.21/-2.28	0.00/0.00
β_x/β_y [mm/mrad]	21.80/15.01	7.18/7.13
$\varepsilon_x/\varepsilon_y$ [mm.mrad]	0.509/0.510	0.256/1.144

TABLE II. The lattice of the EMTEX beam line.

Element	Effective Length [mm]	Gradient [Tesla/m]
Drift	240.5	
Quad	319.0	7.276
Drift	203.0	
Quad	319.0	-7.726
Drift	4000.0	
Quad	354.0	-0.187
Drift	167.5	
Quad	354.0	3.287
Drift	500.0	
Drift	300.0	
Solenoid	100.0	1.00 Tesla
Foil	0.0	$20 \mu\text{g}/\text{cm}^2$, $\Delta\varphi=0.226$ mrad
Solenoid	100.0	1.00 Tesla
Drift	300.0	
Drift	200.0	
Quad	319.0	10.600
Drift	201.0	
Quad	319.0	-9.453
Drift	201.0	
Quad	319.0	8.386
Drift	500.0	
Skew Quad	200.0	-5.618
Drift	20.0	
Skew Quad	400.0	2.840
Drift	20.0	
Skew Quad	200.0	-9.106
Drift	500.0	
Quad	200.0	-6.813
Drift	20.0	
Quad	400.0	7.356
Drift	20.0	
Quad	200.0	-7.760
Drift	1289.0	

MeV/u is stripped in a foil to a $3D_2^+$ beam. The total relative momentum spread is less than $\pm 5 \times 10^{-4}$. The parameters of the full beam line are listed in Tab. II. Positive gradient means horizontal focusing and a skew refer to a normal quadrupole rotated counter-clockwise by 45° around the beam line axis.

-
- [1] D. Edwards, H. Edwards, N. Holtkamp, S. Nagaitsev, J. Santucci, R. Brinkmann, K. Desler, K. Flöttmann, I. Bohnet, and M. Ferrario, in *Proceedings of the XX Linear Accelerator Conference, Monterey, CA*, edited by A. Chao, e000842 (2000).
- [2] B.E. Carlsten, K. Bishofberger, L.D. Duffy, S.J. Russell, R.D. Ryne, N.A. Yampolsky, and A.J. Dragt, *Phys. Rev. ST Accel. Beams* **14**, 034002 (2011).
- [3] B.E. Carlsten, K. Bishofberger, S.J. Russell, R.D. Ryne, and N.A. Yampolsky, *Phys. Rev. ST Accel. Beams* **14**, 084403 (2011).
- [4] P. Piot, Y.-E. Sun, J.G. Power, and M. Rihaoui; *Phys. Rev. ST Accel. Beams* **14**, 022801 (2011).
- [5] Y.-E. Sun, P. Piot, A. Johnson, A.H. Lumpkin, T.J. Maxwell, J. Ruan, and R. Thurman-Keup, *Phys. Rev. Lett.* **105**, 234801, (2010).
- [6] D. Xiang and A. Chao, *Phys. Rev. ST Accel. Beams* **14**, 114001, (2011).
- [7] A. Borov, Proceedings of the 52nd ICFA Advanced Beam Dynamics Workshop, Beijing, PR China, edited by J. Wang (Institute of High Energy Physics, Beijing, PR China, 2012).
- [8] P. Bertrand, J.P. Biarotte; and D. Uriot, in *Proceedings of the 10th European Particle Accelerator Conference, Edinburgh, Scotland*, edited by J. Poole and Christine Petit-Jean-Genaz (Institute of Physics, Edinburgh, Scotland, 2006).
- [9] A.J. Dragt, *Phys. Rev. A* **45**, 4 (1992).
- [10] L. Groening, *Phys. Rev. ST Accel. Beams* **14**, 064201 (2011).
- [11] W. Barth et al., *Proc. XXIV Linac Conf.*, p. 175, (2008).
- [12] The non-symplecticity is from omission of parts of the full system comprising the stripping process. It includes the incoming beam particle nuclei, their residual electrons, and the nuclei and electrons of the stripping foil atoms. However, for the beam dynamics just the stripped beam ions are kept in the system. The stripping atoms and the stripped-off electrons are removed artificially from the system. This removal is non-symplectic.
- [13] <http://web-docs.gsi.de/~weick/atima/>.
- [14] P. Ostroumov, TRACK version-37 user manual, <http://www.phy.anl.gov/atlas/TRACK/>.
- [15] Opera-3D version 15, <http://www.cobham.com>.
- [16] C. Xiao, L. Groening, and O. Kester, Transverse Emittance Transfer, Internal Report IAP-DYNA-190412, Goethe University Frankfurt, Institute of Applied Physics, Frankfurt, Germany (2012).
- [17] C. Xiao, L. Groening, and O. Kester, Proceedings of the 52nd ICFA Advanced Beam Dynamics Workshop, Beijing, PR China, edited by J. Wang (Institute of High Energy Physics, Beijing, PR China, 2012).
- [18] A. Burov, S. Nagaitsev, A. Shemyakin, and Ya. Derbenev, *Phys. Rev. ST Accel. Beams* **3**, 094002 (2000).
- [19] A. Burov, S. Nagaitsev, and Ya. Derbenev, *Phys. Rev. E* **66**, 016503 (2002).
- [20] K.-J. Kim, *Phys. Rev. ST Accel. Beams* **6**, 104002 (2003).